

Abstract. Using the Plateau de Bure Interferometer and IRAM 30m Telescope, we observed λ 2-3mm absorption lines of CS, SO, SO₂, H₂S and HCS⁺ from some of the diffuse clouds which occult our well-studied sample of compact extragalactic mm-wave continuum sources. Our observations of SO, H₂S and HCS⁺ represent the first detections of these species in diffuse clouds; SO₂ was not detected at all. We find a typical value $N(\text{CS}) \approx 0.5 - 2.0 \times 10^{12} \text{ cm}^{-2}$ which is actually much smaller than the values derived previously, along very different lines of sight, from interpretation of CS J=2-1 emission lines. CS forms somewhat sluggishly and is occasionally absent even in features with appreciable $N(\text{HCO}^+)$. But for lines of sight where CS is found, $N(\text{CS})/N(\text{HCO}^+) \approx 2 \pm 1$ or $X(\text{CS}) \approx 4 \times 10^{-9}$. $N(\text{CS})$ correlates well and varies about linearly with $N(\text{HCN})$ ($N(\text{CS})/N(\text{HCN}) = 0.7 \pm 0.3$) though, again, lines of sight with appreciable $N(\text{HCN})$ occasionally lack CS. CS correlates well with H₂S ($N(\text{CS})/N(\text{H}_2\text{S}) = 6 \pm 1$) and marginally with SO ($N(\text{CS})/N(\text{SO}) = 1.7 \pm 0.8$). For the two high column density features observed toward 3C111 we find $N(\text{CS})/N(\text{HCS}^+) = 13.3 \pm 1.0$. CS can easily be shown to form from the observed amounts of HCS⁺ *via* electron recombination in cool, quiescent gas but the obvious gas-phase routes to formation of HCS⁺ fail by factors of 25 or more.

Key words: interstellar medium – molecules

Comparative Chemistry of Diffuse Clouds III: Sulfur-bearing Molecules

R. Lucas¹ and H. S. Liszt²

¹ Institut de Radioastronomie Millimétrique, 300 Rue de la Piscine, F-38406 Saint Martin d'Hères, France

² National Radio Astronomy Observatory, 520 Edgemont Road, Charlottesville, VA, USA 22903-2475

received November 17, 2018

1. Introduction.

This is the third in a continuing series of papers setting forth the run of molecular abundances derived from the mm-wave absorption spectra of diffuse clouds ($A_V \lesssim 1$). For the most part the abundances traced in this work are unexpectedly large, and the species – polyatomic – are of a complexity which is unexpected for a medium threaded by the harsh interstellar radiation field (Drdla et al., 1989). For reasons which are not presently understood, neither the comparatively low density of these regions nor the absence of shielding by dust is a substantial barrier to chemical complexity. Many of these clouds are only barely dense enough or opaque enough to support large abundances of molecular hydrogen and they are marked by an absence of appreciable mm-wave molecular emission in any species beside CO (Liszt & Lucas, 2000). Even CO is occasionally absent in emission despite the clear presence of an absorption feature (Liszt & Lucas, 1998).

The two earlier papers in this series concerned families of molecules whose presence in the interstellar medium first became known when their simplest, diatomic members (CH, CN) appeared in absorption toward nearby bright stars ¹ In Paper I (Lucas & Liszt, 2000) we considered the C_nH_m species CH, C_2H , C_3H_2 etc.. We showed that C_2H is widespread – detectable in every feature seen in HCO^+ , with $N(C_2H)/N(HCO^+)$ higher at small $N(HCO^+)$ or $N(H_2)$ – and about linearly related in column density to C_3H_2 . C_3H_2 was already known to be ubiquitous from prior work at cm-wavelengths (Cox et al., 1988).

In Paper II we examined the cyanogen-bearing species CN, HCN, and HNC (Lucas & Liszt, 2000; Liszt & Lucas, 2000) and discovered a very tight linear proportionality among the column densities of all three of these species, analogous to what we had seen previously between for OH and HCO^+ . This enabled another calibration of the molecular abundance scale based on the existing body of

optical/*uv* absorption work relating $N(CN)$ and $N(H_2)$ along a few lines of sight. From the fact that the CN-family abundances vary with $N(H_2)$ at nearly fixed values of the total visual extinction along those lines of sight, we inferred (after modelling the formation of H_2 in diffuse gas of varying number and column density) that the trace molecules increase in quantity and abundance even as H_2 itself does.

In this work we address the sulfur-bearing molecules CS, SO, H_2S , HCS^+ and SO_2 whose presence in the interstellar medium was only found later, through mm-wavelength emission originating in GMC's and dark molecular clouds. With the possible exception of CS, the first four of these species have been entirely unknown in the diffuse gas until the present work, and conventional gas-phase ion-chemistry models predict that they should not exist in detectable quantities there (see Sect. 4). The sulfur-bearing molecules are exceptionally interesting species to detect in the diffuse environment because models of their gas-phase chemistry in translucent, dark and dense clouds appear to fail in rather spectacular fashion; OH and/or O_2 are required to be overabundant, compared to direct observation, by very large factors (20 - 200) in order to explain even the simpler species like CS and SO (see Sect. 5.1).

More generally, though it is often claimed that models of quiescent gas-phase ion-molecule chemistry can reproduce (or nearly so) the abundances of simpler group members like CH, CN, CS, or OH in diffuse clouds (although not CO), it usually transpires that these same models do not come close to explaining the abundances of polyatomics like HCN, HCO^+ , HCS^+ , etc. from which the diatomics form *via* photodissociation or dissociative recombination in diffuse gas. Thus the ability of simple models to explain the various diatomics is at best somewhat accidental and a deeper explanation of the full panoply of observed species is needed.

The plan of the present work is as follows. The manner of taking and analyzing the present observations is discussed in Sect. 2. The main observational results of this work are discussed in Sect. 3. Sect. 4 reviews the prior history of observations of sulfur-bearing species in the in-

Send offprint requests to: H. S. Liszt

Correspondence to: hlszt@nrao.edu

¹ Another possible family, starting with OH and HCO^+ and leading to CO, has been the subject of much of our prior work (Lucas & Liszt, 1996; Liszt & Lucas, 1996, 2000).

Table 1. Background sources and profile rms

Source	l °	b °	$\sigma_{l/c}$ CS	$\sigma_{l/c}$ SO	$\sigma_{l/c}$ H ₂ S
B0212+735	128.93	11.96	0.046	0.021	
B0355+508	150.38	-1.60	0.045	0.014	0.110
B0415+379	161.68	-8.82	0.029	0.028	0.055
B0528+134	191.37	-11.01	0.032	0.018	
B1730-130	12.03	+10.81	0.021	0.018	
B2200+420	92.13	-10.40	0.022	0.027	0.047
B2251+158	86.11	-38.18	0.006		

Table 2. Species and lines observed

Species	line	frequency MHz	resolution km s ⁻¹	factor ¹
CS	2 – 1	97981	0.428	8.06
SO	3 ₂ – 2 ₁	99300	0.423	28.6
SO ₂	3 ₁₃ – 2 ₀₂	104029	0.403	26.3
H ₂ S	1 ₁₀ – 1 ₀₁	168763	0.249	1.80
HCS ⁺	2 – 1	85348	0.492	12.9

¹ units are 10¹² cm⁻²(km s⁻¹)⁻¹

terstellar medium and Sect. 5 discusses extant models and theory. Sect. 6 is a brief discussion and Sect. 7 a summary.

2. Observations.

Table 1 lists the background sources observed, along with their galactic coordinates and (for some of the transitions) the rms noise levels achieved in the line/continuum ratio, which is the rms error in optical depth in the optically-thin limit. H₂S and SO₂ were observed toward B0355+508, B0415+379, and B2200+379 at the IRAM 30m telescope in 1995 January and November using beam-switching. CS, SO, and HCS⁺ were observed at the Plateau de Bure interferometer in many sessions during the years 1993-1997 and the mode of observation was identical to that described previously by Lucas & Liszt (2000) and in our other prior work. The beam-switched observations at the 30m are straightforward because there is no emission of any significance in the foreground gas. All data were taken with a channel separation of 78.1 kHz and a channel width (FWHM) of 140 kHz, corresponding to velocity intervals which are tabulated for the various individual species.

Table 2 gives the species and transitions observed, along with the velocity resolution (corresponding to 140 kHz) and the factor by which the measured integrated optical depths were scaled to derive the total column density. As is usual for species having higher dipole moments (than CO), we evaluate the rotational partition function by assuming that the populations are in equilibrium with the cosmic microwave background. This follows from the diffuse nature of the host gas and its consequent inability to support substantial rotational excitation in any species beside CO, even when the electron excitation is included. As we have noted (see, for example, Liszt & Lucas (2000)), of

all the species with appreciable dipole moments (typically 2-4 Debye), only HCO⁺ has been detected in emission toward our sources and it is exceedingly weak even when the optical depth is high. We have never succeeded in detecting CS emission and the thermal pressures indicated by CO absorption profiles also show that the weak-excitation limit is appropriate (Liszt & Lucas, 1998). The CS emission observed by Drdla et al. (1989) is consistent with this assumption, as well.

2.1. Component fitting and profile integrals

We did not attempt a comprehensive regimen of fitting Gaussian components to the sulfur-molecule profiles such as we did in prior work, because, frankly, the data discussed here are older and generally of lower quality. Instead, for all lines of sight except B0415+379 (where the profile integrals arise from gaussian decomposition), we simply blocked out regions of the profiles according to the component structure gleaned from prior experience with HCO⁺, C₂H, HCN, *etc.*, and integrated over these regions. The basic data from which our Figures and conclusions were drawn are given in the Appendix.

3. Systematics

3.1. *N*(CS) and variation across chemical families

Figure 4 compares the variation of the CS column density (by far the most widely-observed species) with those of representatives of the other chemical families we have studied. Although it is HCO⁺ whose abundance relative to H₂ is the most nearly constant, and although N(H₂) increases to the right in Fig. 5, it is not necessarily the case that variations in A_V dominate the changes in molecular column density, as shown in Paper II. More likely, it is some combination of higher total number density and extinction which drives the molecular fraction higher in both H₂ and the trace species.

Although CS is occasionally found in features of low molecular column density, it is also occasionally absent at intermediate values of N(HCO⁺), *etc.* The tightest correlation, and the most nearly linear power-law slope, is found between N(CS) and N(HCN). Again, this represents a functional dependence – the two species are affected in similar ways by changes in whatever are the independent variables – not necessarily a causal relationship. Typical values of N(CS) are N(CS) ≈ 1 – 2 × 10¹² cm⁻², N(CS)/N(HCO⁺) ≈ 2 ± 1, averaged unweighted over all features where both species were detected. For those features where both CS and another species were detected, N(CS)/N(HCN) = 0.7 ± 0.3, N(CS)/N(C₂H) = 0.13 ± 0.07.

3.2. Abundance ratios of sulfur-bearing species

Figures 2, 3 and 5 detail the presence of SO and H₂S in several features having relatively high N(CS). We find

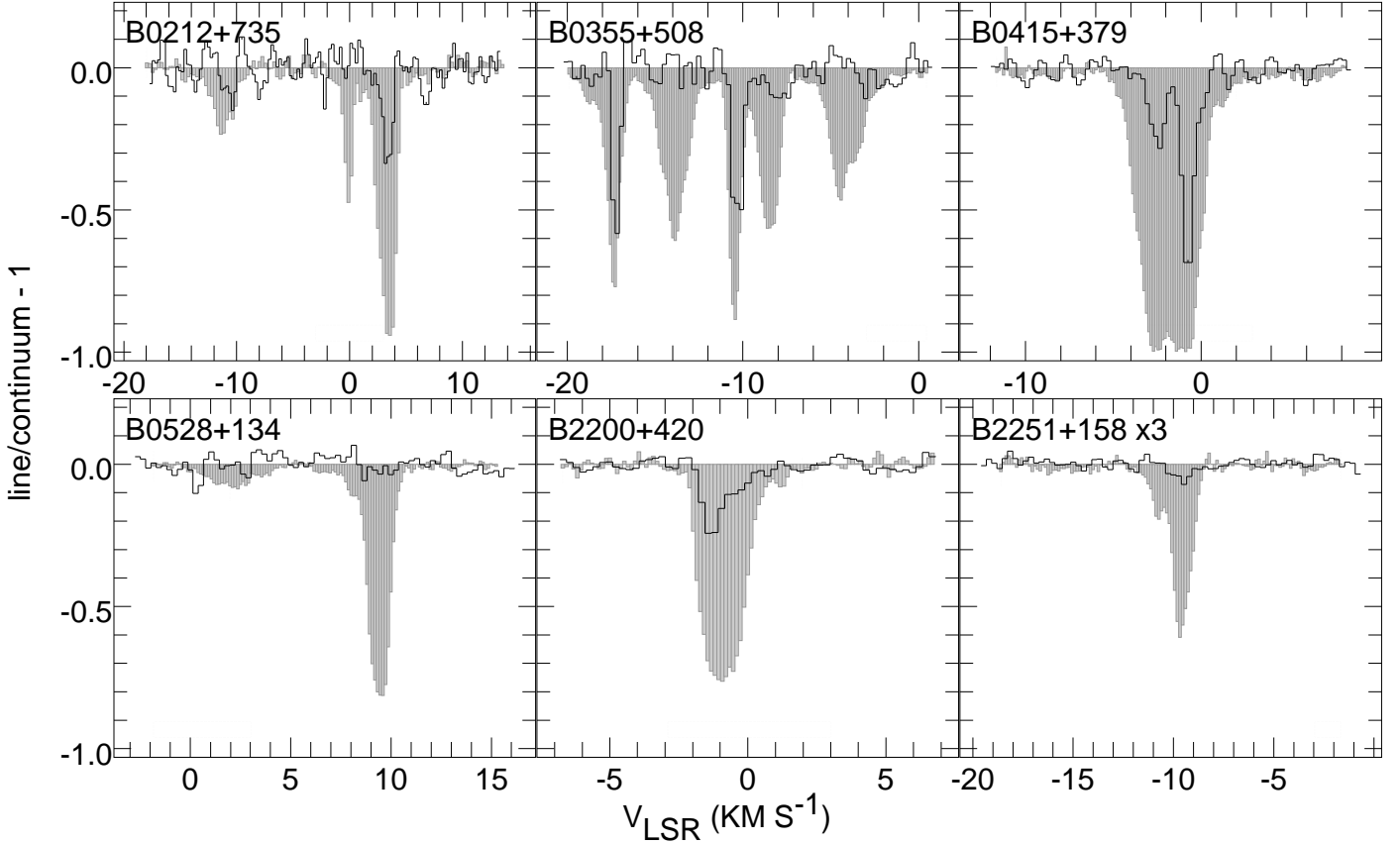


Fig. 1. CS J=2-1 (histogram) and HCO⁺ J=1-0 (gray overlay) absorption spectra toward six sources showing all the detected CS components and the barren spectrum toward B0528+134.

$N(\text{CS})/N(\text{H}_2\text{S}) = 6 \pm 1$ and $N(\text{CS})/N(\text{SO}) = 1.7 \pm 0.8$. Of the seven features with $N(\text{CS}) > 10^{12} \text{ cm}^{-2}$ in Fig. 5, only two have $N(\text{SO})/N(\text{CS})$ above unity, ≈ 1.3 . For the two high column density features observed toward 3C111 which show HCS⁺ we find ratios $N(\text{CS})/N(\text{HCS}^+) = 11.1 \pm 2.0$ and 14.2 ± 1.3 or a weighted mean ratio $N(\text{CS})/N(\text{HCS}^+) = 13.3 \pm 1.0$. Abundances of the sulfur-bearing species all tend to increase together but only between CS and H₂S do the limited data show a strong and clear correlation.

3.3. SO₂

SO₂ was the only molecule sought which was not detected and its abundance is only loosely constrained by the present work. The upper limit on the relative abundance of SO₂ shown in Table 3 is typical.

4. Prior observations and discussions of sulfur chemistry in diffuse clouds

Observationally, Snow's *Copernicus* limits on SH toward *o* Per, $N(\text{SH}) < 10^{12} \text{ cm}^{-2}$ (Snow, 1975), and on CS toward ζ Oph, $N(\text{CS}) < 2.6 \times 10^{13} \text{ cm}^{-2}$ (Snow, 1976), constituted the entire body of knowledge of sulfur chemistry in diffuse

clouds for some time. Ferlet et al. (1986) then showed that $N(\text{CS}^+) < 1.9 \times 10^{11} \text{ cm}^{-2}$ toward ζ Oph, amending an earlier, tentative detection. Eventually, Drdla et al. (1989) detected very weak (0.01 - 0.10 K) CS J=2-1 emission toward several objects occulted by supposedly diffuse gas ($A_V \lesssim 1 \text{ mag}$), including *o* Per and HD210121 ($T_A^* = 0.03 - 0.04 \text{ K}$, $N(\text{CS}) = 4 - 100 \times 10^{12} \text{ cm}^{-2}$, $N(\text{CS})/N(\text{H}_2) \geq 0.4 - 10 \times 10^{-8}$), and (somewhat tentatively) ζ Oph ($T_A^* = 0.01 \text{ K}$, $N(\text{CS}) = 0.7 - 5 \times 10^{12} \text{ cm}^{-2}$, $N(\text{CS})/N(\text{H}_2) = 0.15 - 1.1 \times 10^{-8}$).

The large ranges in derived CS column density in the work of Drdla et al. (1989) reflect a sensitivity to the assumed physical conditions, but the implied relative abundances are really very high – in fact, quite comparable to or even larger than those found in dark clouds and GMC's.² Nonetheless, Drdla et al. (1989) concluded that CS could be made in the required amount by ordinary gas-phase ion-molecule chemistry acting in quiescent diffuse/translucent gas with $n(\text{H}) = 200 - 1000 \text{ cm}^{-3}$ and $T_K = 30 - 50 \text{ K}$, and they predicted (for the line of sight

² As is evident from our work, where the typical CS column density is $N(\text{CS}) = 1 - 2 \times 10^{12} \text{ cm}^{-2}$, the higher CS abundances found by Drdla et al. (1989) suggest that either the density was underestimated or that the gas sampled in emission is considerably less diffuse than was believed at the time.

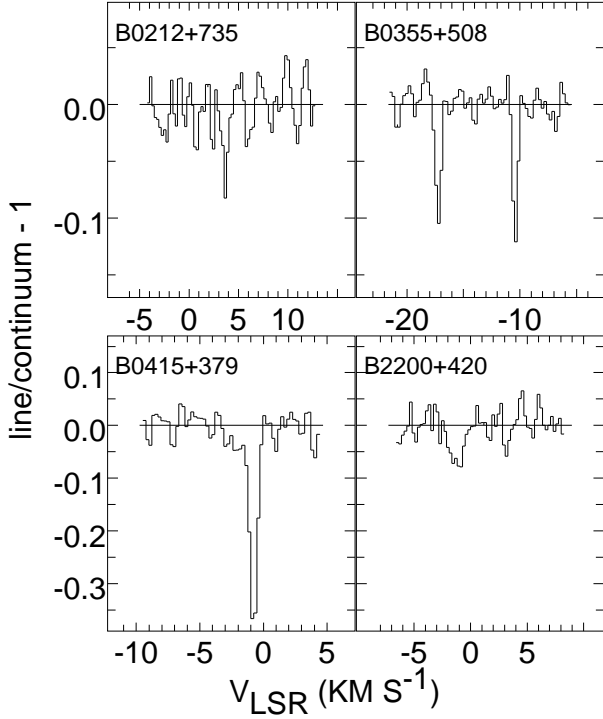


Fig. 2. Digest of detected SO absorption features.

toward ζ Oph) the diffuse-cloud abundances of some of the other sulfur-bearing species known to exist in molecular clouds, *i.e.* $N(\text{CS})/N(\text{HCS}^+) = 40 - 80$, $N(\text{CS})/N(\text{SO}) = 2800 - 3800$, $N(\text{CS})/N(\text{H}_2\text{S}) \approx N(\text{CS})/N(\text{SO}_2) \approx 10^9$. For these ratios, the observed values from the present data (along other directions) are 13, 2, 6, and > 2 .

4.1. CS emission toward ζ Oph

We tried and failed (see Liszt (1997)) to confirm the interesting but somewhat tentative detection of 0.013 ± 0.003 K CS $J=2-1$ emission at the somewhat unusual velocity of -1.29 km s^{-1} toward ζ Oph by Drdla et al. (1989). Our spectra of HCO^+ and CS at two positions are shown in Fig. 6. At the HCO^+ emission peak $30'$ South of the star, CS emission is at least an order of magnitude weaker than that of HCO^+ . If this proportionality were preserved, CS emission toward the star would be six times weaker than claimed by Drdla et al. (1989). Toward the star, the 1σ rms fluctuation in integrated CS line intensity in our data is $0.005 \text{ K km s}^{-1}$, but there is no signal. So the 4σ integrated intensity detection quoted by Drdla et al. (1989), $I_{\text{CS}} = 0.020 \pm 0.005 \text{ K km s}^{-1}$, is a 4σ upper limit in our data.

5. Models for sulfur chemistry

As is usual for the results presented in this series of papers, the relative abundances are similar to those believed to obtain in dark clouds (Table 3). The theoretical sulfur chemistry of dark and dense clouds is generally (but

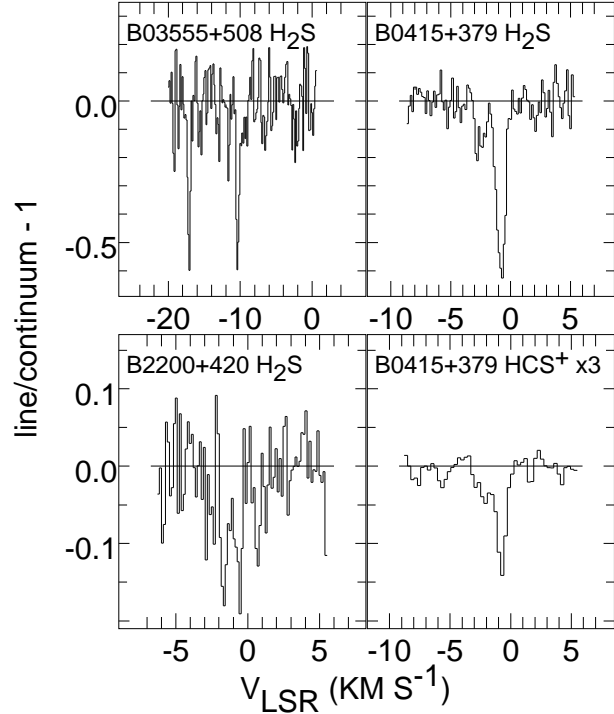


Fig. 3. Digest of detected H_2S and (lower right) HCS^+ absorption features. The HCS^+ profile has been scaled upward by a factor 3.

not obviously correctly) considered to be on a firmer footing than that for diffuse gas and is discussed first in this Section.

5.1. Dark gas

Sulfur chemistry is conditioned on the inability of all species SH_n^+ ($n = 0, 1, \dots$) to protonate in reaction with H_2 at low temperatures (*i.e.* $\text{S}^+ + \text{H}_2 + 9860 \text{ K} \rightarrow \text{SH}^+ + \text{H}$); these reactions are all much more endothermic even than, say, $\text{C}^+ + \text{H}_2 + 4640 \text{ K} \rightarrow \text{CH}^+ + \text{H}$, and $\text{CH}^+ + \text{H}_2$ is exothermic. Because of this, quiescent dark and dense cloud gas-phase ion-molecule chemistry is usually understood as making SO *via* the reaction of S with OH and/or O_2 , $\text{S} + \text{OX} \rightarrow \text{SO} + \text{X}$, while CS forms partly from $\text{C} + \text{SO} \rightarrow \text{CS} + \text{O}$ (an important sink for SO) and partly from another chain initiated by S^+ , such as $\text{S}^+ + \text{CH} \rightarrow \text{CS}^+ + \text{H}$ (Oppenheimer & Dalgarno, 1974; Nillson et al., 2000). CS, in its turn, is destroyed in the reaction $\text{CS} + \text{O} \rightarrow \text{CO} + \text{S}$.

The importance of reactions with free atomic oxygen and carbon renders the CS/SO ratio in dark gas highly dependent on the elemental abundance ratio of O and C, and also to the extent to which these are converted to CO. A higher O/C ratio leaves more free gas-phase atomic oxygen (after CO is formed) resulting in higher abundances of OH and O_2 , more rapid SO formation and CS destruction

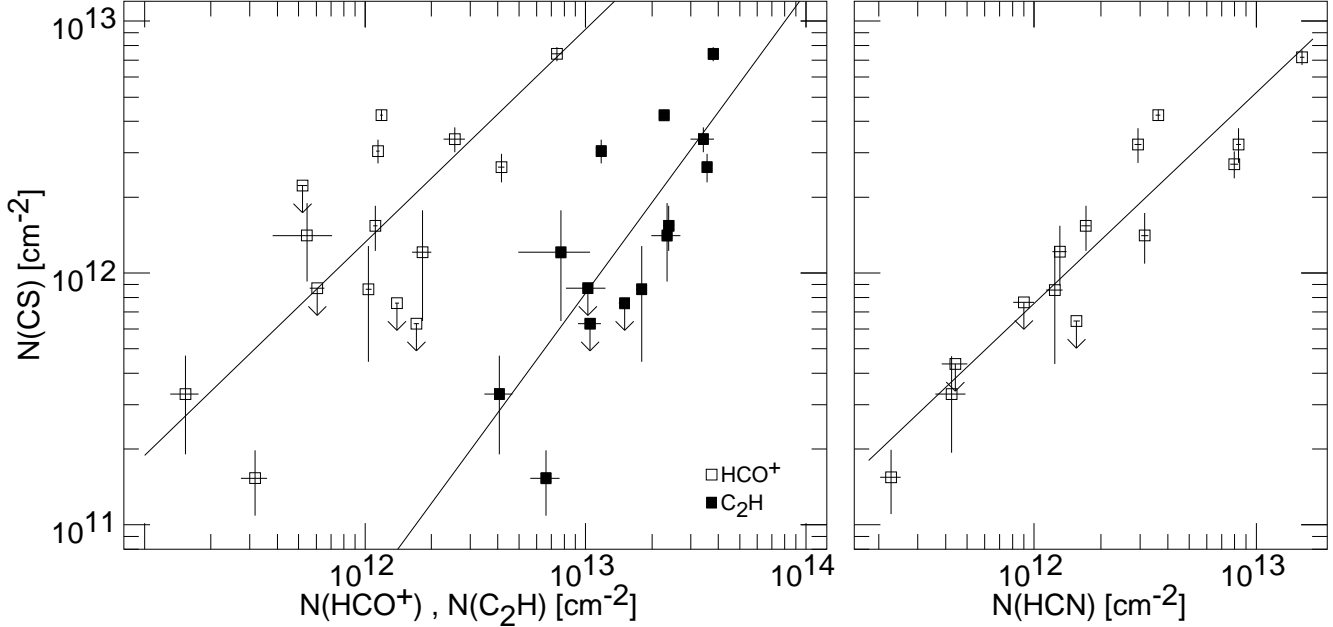


Fig. 4. Variation of $N(\text{CS})$ with $N(\text{HCO}^+)$, $N(\text{C}_2\text{H})$, and $N(\text{HCN})$. The power-law slopes for lines of sight with detections, is 0.84 ± 0.20 for CS and HCO^+ ; 1.2 ± 0.3 for CS and C_2H and 0.84 ± 0.09 for CS and HCN. Also for lines of sight with detections, we have $\langle \text{CS}/\text{HCO}^+ \rangle = 1.57 \pm 0.97$, $\langle \text{CS}/\text{C}_2\text{H} \rangle = 0.11 \pm 0.07$ and $\langle \text{CS}/\text{HCN} \rangle = 0.72 \pm 0.28$.

and a larger SO/CS ratio (see Fig. 3c of Gerin et al. (1997) which also includes the data of Turner (1995, 1996)).

SO also combines with O and OH to form SO_2 so the O/C ratio affects the balance between SO and SO_2 . In time-dependent models it is seen that SO_2 is one of the most extreme of the “late-type” species, which appear in substantial quantities late in the chemical evolution of an initially diffuse gas. In this regard it is similar to NH_3 and to N_2H^+ (Watt & Charnley, 1985). In general, the amounts of OH and/or O_2 which are needed to reproduce the observed quantities of sulfur-bearing species in dark and dense clouds are far higher than those which are actually observed. When gas-grain coupling is considered, high OH abundances lead to a late-time “accretion catastrophe” (Charnley et al., 2001) whereby sulfur is lost to the gas-phase entirely.

Nillson et al. (2000) have modelled the gas-phase ion-molecule chemistry in dense clouds and find that the very appreciable variations in mean SO/CS ratio between sources can be explained by factor two variations in the O/C ratio in the gas; spatial variations in the SO/CS ratio across individual sources are then to be understood in terms of density structure and other local behaviour. They noted that their models entail overproduction of O_2 by very large factors as compared to existing observations, and suggested that future searches for the elusive O_2 molecule might best be focused on lines of sight where the problems of sulfur chemistry were most severe in this regard. Earlier, Turner (1995, 1996) encountered similar difficulties in attempting to account for the abundances of sulfur-bearing species in translucent clouds,

Table 3. Abundances relative to HCO^+

Species	This work	TMC-1	L134N
HCO^+	1.0	1.0	1.0
CS	1.6	1.3	0.13
SO	0.9	0.63	2.5
SO_2	< 0.5	< 0.13	0.5
H_2S	0.27	0.09	0.10
HCS^+	0.13	0.08	0.008
HCN	2.3	2.5	0.5
C_2H	13	6-12	< 6

“This work” represents this work and data from Papers 1 and 2 for C_2H and HCN. Results for TMC-1 are taken from Ohishi et al. (1992) and (for H_2S) Minh et al. (1989); L134N data are from Ohishi et al. (1992). The abundance of HCO^+ relative to H_2 is given by Ohishi et al. (1992) as 0.8×10^{-8} for either dark cloud while a somewhat lower value 0.2×10^{-8} is indicated for diffuse gas (Liszt & Lucas, 2000).

where the required OH fractional abundance was found to be 2×10^{-5} , again much higher than the values typically seen at $A_V < 7$ mag, which are (with little variation) about 10^{-7} (Crutcher, 1979; Turner & Heiles, 1974).

5.2. Diffuse gas

Early-on, Duley et al. (1980) noted that SO and SH (but not H_2S) might be formed in diffuse clouds if the radiative association of S^+ and H_2 occurred sufficiently rapidly. They hypothesized that the presence of sulfur-bearing compounds in diffuse gas, if demonstrated, might then point either to the efficacy of this reaction or to the impor-

tance of grain chemistry and gas-grain coupling. Slightly later, but at a time when sulfur-bearing species had still not yet been observed in diffuse clouds, Pineau Des Forets et al. (1986) showed that high abundances of CS, $N(\text{CS}) \geq 10^{12} \text{ cm}^{-2}$, or $N(\text{CS})/N(\text{HCS}^+)$ and $N(\text{CS})/N(\text{H}_2\text{S})$ ratios of order unity, could be produced in the same strong (10 km s^{-1}) MHD shocks which seemed required to reproduce $N(\text{CH}^+)$. They suggested that SH^+ might be observable. Similar effects enhancing the abundance of sulfur-bearing molecules in shocked dense gas were shown by Mitchell (1984).

Drdla et al. (1989) criticized the prior conclusions of both Duley et al. (1980) and Pineau Des Forets et al. (1986), arguing that the abundances predicted by the shock and grain models would not have been any higher than those of steady-state gas-phase chemistry, had the interstellar photoionization rates had not been underestimated. They modelled quiescent gas-phase sulfur chemistry, as cited here in Sect. 4, and discussed the formation of CS (whose emission they observed) *via* the interactions of S^+ with CH and C_2 (whose abundances are well-determined) to form CS^+ , HCS^+ and CS (via the recombination of HCS^+). They concluded that the formation of CS from HCS^+ could be modelled if some favorable adjustments to the CS^+ formation rates and CS photodestruction rates were made.

It is a fairly straightforward exercise to show that the relative abundance of HCS^+ seen in this work (Table 3 with $X(\text{HCO}^+) \equiv N(\text{HCO}^+)/N(\text{H}_2) = 2 \times 10^{-9}$) easily suffices to reproduce the observed CS column densities without any of the favorable adjustments to rate constants and photo-dissociation rates discussed by Drdla et al. (1989). That is, for a diffuse gas having an electron fraction $X(\text{e}) = 2 \times 10^{-4}$ and using the standard CS photodestruction (10^{-9} s^{-1}) and HCS^+ recombination rates found in the UMIST reaction database, we find $X(\text{CS}) = 1.4 \times 10^{-11} n(\text{H}_2)(30/T_K)^{0.75}$ in free space.

However, the converse is not true; the observed diffuse gas abundances of the species supposedly contributing to the formation of HCS^+ ($X(\text{S}^+) = 3 \times 10^{-5}$; $X(\text{CH}) = 4 \times 10^{-8}$; $X(\text{C}_2) = 2.4 \times 10^{-8}$) fall a factor of 10-20 short using quiescent gas-phase chemical rates (the situation is far less favorable for the other species, as mentioned in Sect. 4). This situation is essentially identical to that for CO, where the observed amounts of HCO^+ can easily recombine under typical quiescent conditions to reproduce $N(\text{CO})$, but the most likely progenitors of HCO^+ (OH and C^+), both having measured abundances in at least some cases, fall similarly short of explaining the required column density $N(\text{HCO}^+)$ (Liszt & Lucas, 2000). In principle this line of argument could be extended to the CN-HCN-HNC family but the permanent dipole moment of HCNH^+ is small and the experiment is somewhat challenging for current instruments.

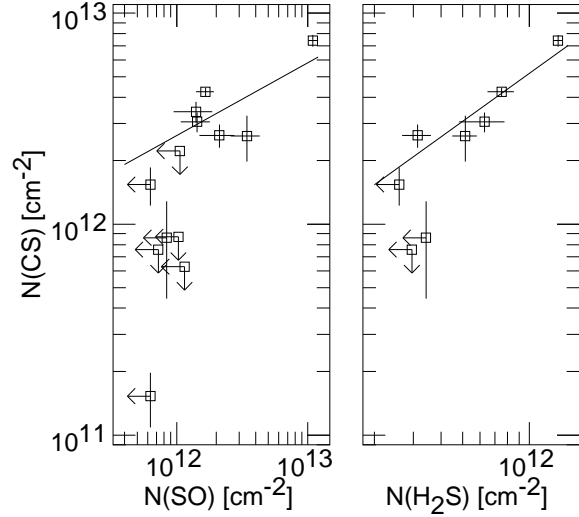


Fig. 5. Variation of $N(\text{CS})$ with $N(\text{SO})$, $N(\text{H}_2\text{S})$.

6. Discussion

Table 3 presents a comparison of relative abundances between the diffuse gas observed here and representative results for the well-studied dark clouds TMC-1 and L134N. It should be noted that there are large variations in the CS/SO ratio between and within individual dense sources observed in emission (including these two dark clouds) and that TMC-1 and L134N, whose CS/SO ratios differ by about a factor 40, represent the extremes of the observed range (Nillson et al., 2000; Gerin et al., 1997). The abundances of CS and HCO^+ relative to H_2 in diffuse clouds are about 25%-50% that inferred for TMC-1.

The abundance ratios relative to HCO^+ are essentially identical for our sample of diffuse clouds and the representative conditions quoted for TMC-1, with the possible exception of an overabundance of H_2S in our objects. For the dense clouds and GMC studied by Nillson et al. (2000), the typical SO/CS ratio is 0.2 (i.e. it is TMC-1-like) with only one-fifth at or above unity; this is just what is seen in diffuse clouds as well. But for translucent and dark clouds, ratios $\text{SO}/\text{CS} < 1$ are actually the exception as detailed in Fig. 3c of Gerin et al. (1997) which includes the data collected by Turner (1995, 1996).

It is now possible to make comparisons of the abundances of several species which differ in structure by the replacement of one atom with that of a different element, as for example HCS^+ and HCO^+ , or CS and SO, *etc.* Table 4 points out that these abundance ratios are not very different from that of the elements which are exchanged, the outstanding exception being the CH/NH ratio which is substantially greater than either C_2/CN or $\text{C}_2\text{H}/\text{HCN}$.

7. Summary

A full complement of sulfur-bearing molecules may be found in diffuse or low-extinction gas using mm-wave ab-

Table 4. Elemental and Molecular abundance ratios

Ratio	Solar	ζ Oph	Species	Diffuse
C/O	0.50	0.50	CS/SO	1.7 ± 0.8
			CH/OH	0.48, 0.52, 0.24
C/N	3.80	1.74	CH/NH	22, 28
			C ₂ /CN	9
			C ₂ H/HCN	5
S/O	0.025	0.10	HCS ⁺ /HCO ⁺	0.055, 0.070
S/N	0.20	0.36	CS/CN	0.1 ± 0.05

ζ Oph elemental abundances from Savage and Sembach (1996)

OH and CH abundances from Van Dishoeck & Black (1986)

NH from Crawford & Williams (1997) and Meyer & Roth (1991)

C₂/CN from Federman et al. (1994), see Paper II, Fig. 3

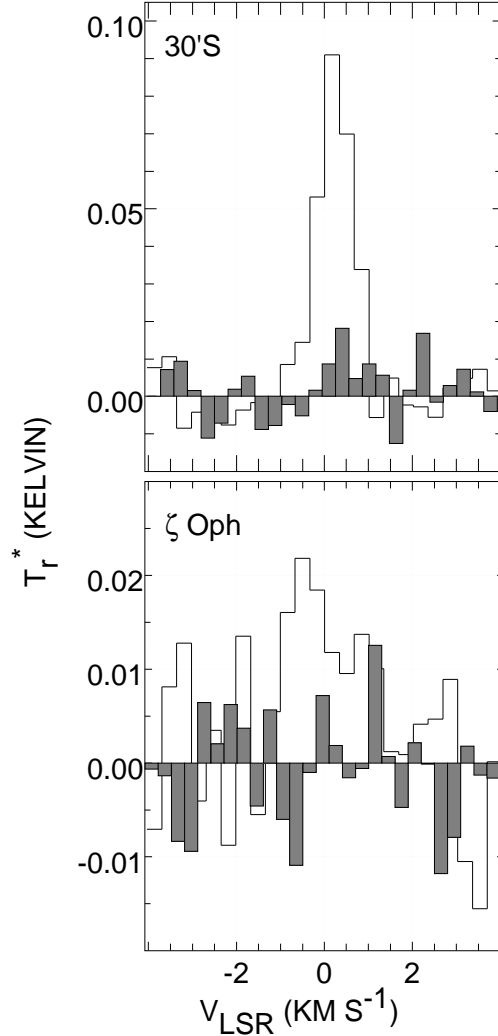
sorption techniques, including CS, SO, H₂S and HCS⁺. Only the first of these might have been seen prior to our work; we actually find much lower CS abundances than were derived earlier from observations of weak J=2-1 emission in objects purported to have A_V of order unity. The observed high abundances of SO, H₂S and HCS⁺ cannot be reproduced by any gas-phase ion-molecule chemistry in quiescent diffuse gas, or perhaps even in much denser dark and translucent gas as well: there is a general consensus that the relative abundances of OH and/or O₂ required to explain the sulfur chemistry of dark gas are grossly out of line with what is actually observed.

The column density of HCS⁺ detected along one line of sight is entirely sufficient to explain the observed CS column density *via* ordinary dissociative recombination at the standard (though very uncertain) free-space CS photodissociation rate. This is analogous to the situation for HCO⁺ and CO, which requires a somewhat more elaborate calculation of the photodissociation rate but for which there is much more data. In both cases, the likely precursors of the ion have relatively well-determined abundances and the inferred formation rate is 1-2 orders of magnitude too small under quiescent conditions.

The abundances of the sulfur-bearing molecules seem consistent with the predictions of MHD shock models but the kinematics of shock models are never evident in our line profiles for any species. In general, it is clear that some mechanism is putting energy into either the gas or the reactions; macroscopic shock models do this explicitly but not acceptably.

The next paper in this series will discuss old optical and new microwave measurements of the CH radical.

Acknowledgements. The National Radio Astronomy Observatory is operated by AUI, Inc. under a cooperative agreement with the US National Science Foundation. IRAM is operated by CNRS (France), the MPG (Germany) and the IGN (Spain). We owe the staff at IRAM (Grenoble) and the Plateau de Bure our thanks for their assistance in taking the data. We thank the referee, C. M. Walmsley, for helpful comments.

**Fig. 6.** CS J=2-1 (shaded) and HCO⁺ (1-0) emission profiles toward and 30' South of ζ Oph.

References

- Charnley, S. B., Rodgers, S. D., & Ehrenfreund, P. 2001, A&A, 378, 1024
- Cox, P., Guesten, R., & Henkel, C. 1988, A&A, 206, 108
- Crawford, I. A. & Williams, D. A. 1997, Mon. Not. R. Astron. Soc., 291, L53
- Crutcher, R. M. 1979, ApJ, 231, L151
- Drdla, K., Knapp, G. R., & van Dishoeck, E. F. 1989, ApJ, 345, 815
- Duley, W. W., Millar, T. J., & Williams, D. A. 1980, Mon. Not. R. Astron. Soc., 192, 945
- Federman, S. R., Strom, C. J., Lambert, D. L., Cardelli, J. A., Smith, V. V., & Joseph, C. L. 1994, ApJ, 424, 772
- Ferlet, R., Roueff, E., Czarny, J., & Felenbok, P. 1986, A&A, 168, 259
- Gerin, M., Falgarone, E., Joulain, K., Kopp, M., Le Bourlot, J., Pineau Des Forets, G., Roueff, E., & Schilke, P. 1997, A&A, 318, 579

- Liszt, H. S. 1997, *A&A*, 322, 962
Liszt, H. S. & Lucas, R. 1996, *A&A*, 314, 917
—, 1998, *A&A*, 339, 561
—, 2000, *A&A*, 355, 333
Lucas, R. & Liszt, H. S. 1996, *A&A*, 307, 237
—, 2000, *A&A*, 355, 327
Meyer, D. M. & Roth, K. C. 1991, *ApJ*, 376, L49
Minh, Y. C., Irvine, W. M., & Ziurys, L. M. 1989, *ApJ*, 345, L63
Mitchell, G. F. 1984, *ApJ*, 287, 665
Nillson, A., Hjalmarson, P., Bergman, P., & Millar, T. 2000, *A&A*, 358, 257
Ohishi, M., Irvine, W., & Kaifu, N. 1992, in *Astrochemistry of cosmic phenomena: proceedings of the 150th Symposium of the International Astronomical Union*, held at Campos do Jordao, Sao Paulo, Brazil, August 5-9, 1991. Dordrecht: Kluwer 1992, ed. P. D. Singh, 171–172
Oppenheimer, M. & Dalgarno, A. 1974, *ApJ*, 187, 231
Pineau Des Forets, G., Roueff, E., & Flower, D. R. 1986, *Mon. Not. R. Astron. Soc.*, 223, 743
Snow, T. P. 1975, *ApJ*, 201, L21
—, 1976, *ApJ*, 204, L127
Turner, B. E. 1995, *ApJ*, 455, 556
—, 1996, *ApJ*, 461, 246
Turner, B. E. & Heiles, C. E. 1974, *ApJ*, 194, 525
Van Dishoeck, E. F. & Black, J. H. 1986, *Astrophys. J.*, Suppl. Ser., 62, 109
Watt, G. D. & Charnley, S. B. 1985, *Mon. Not. R. Astron. Soc.*, 213, 157

Appendix A: Line profile integrals

Table A.1. Line profile (optical depth) integrals

Source	V km s ⁻¹	HCO ⁺ km s ⁻¹	C ₂ H km s ⁻¹	HCN km s ⁻¹	CS km s ⁻¹
B0212	-8	0.594(0.046)	0.378(0.077)	0.234(0.031)	< 0.11 ¹
	0	0.509(0.026)	0.177(0.056)		< 0.28
	3	2.500(0.281)	1.259(0.150)	4.406(0.107)	0.42(0.05)
B0355	-17	1.120(0.041)	0.434(0.022)	1.555(0.057)	0.38(0.04)
	-14	1.367(0.028)	0.554(0.031)	0.477(0.051)	<0.09
	-10	1.161(0.016)	0.837(0.026)	1.915(0.049)	0.53(0.02)
	-8	1.089(0.025)	0.880(0.032)	0.907(0.045)	0.19(0.04)
	-3	1.016(0.030)	0.662(0.035)	0.655(0.056)	0.11(0.05)
B0415	-2	4.060(0.14)	1.307(0.026)	4.16(0.174)	0.33(0.04)
	-1	7.27(0.37)	1.402(0.02)	8.532(0.212)	0.92(0.06)
B0528	10	1.674(0.046)	0.387(0.046)	0.823(0.027)	<0.08
B1730	all	0.150(0.022)	0.150(0.022)	0.225(0.035)	0.04(0.02)
B2200	-2	0.533(0.16)	0.864(0.13)	1.67(0.063)	0.18(0.06)
	-1	1.78(0.18)	0.285(0.10)	0.690(0.050)	0.15(0.07)
B2251	all	0.31(0.042)	0.244(0.037)	0.120(0.013)	0.02(0.006)

¹ upper limits are 2 σ **Table A.2.** Line profile (optical depth) integrals

Source	V km s ⁻¹	SO km s ⁻¹	SO ₂ km s ⁻¹	H ₂ S km s ⁻¹	HCS ⁺ km s ⁻¹
B0212	-8	< 0.036			
	0	<0.037			
	3	0.049(0.016)			
B0355	-17	0.050(0.013)	<0.066	0.349(0.081)	
	-14	<0.025	<0.066	<0.164	
	-10	0.058(0.009)	<0.045	0.417(0.057)	
	-8	0.022(0.039)	<0.058	<0.144	
	-3	0.0292(0.052)	<0.074	<0.190	
B0415	-2	0.074(0.022)	<0.054	0.174(0.026)	0.0185(0.0024)
	-1	0.381(0.030)	<0.062	0.750(0.035)	0.0405(0.0025)
B0528	10	<0.040			
B2200	-2		< 0.024		
	-1		< 0.025		
	all	0.12±0.03	< 0.035	0.286(0.036)	
B2251	all	< 0.022			